



A Compact Wind Tunnel for Calibrating Anemometers Used for Indoor Airflow

A. Iwai* , N. Kurihara, T. Takatsuji, T. Morioka and T. Shimada

National Institute of Advanced Industrial Science and Technology (AIST), National Metrology Institute of Japan (NMIJ), Tsukuba Central 3, Umezono 1-1-1, Tsukuba 305-8563, Japan

Received: 10 May 2022 / Accepted: 30 March 2023 / Published online: 19 May 2023

© Metrology Society of India 2023

Abstract: In order to evaluate an indoor airflow, which may cause the spread of viruses, it is effective to measure the speed and direction of the airflow using several accurately evaluated anemometers. However, since calibration of anemometers is a time-consuming task, so the authors developed a compact wind tunnel that can evaluate the accuracy of anemometers in a short amount of time. The design concept and performance of the wind tunnel are described by several indices, including averaging time, settling time, spatial distribution, and blockage effect. These results demonstrate the capability of the wind tunnel to evaluate several anemometers in a short measurement time with sufficiently high precision.

Keywords: Windtunnel; Indoor airflow; Anemometer; Calibration; Measurement

1. Introduction

The speed of an indoor airflow is generally low, i.e., less than 1.0 m/s. Compared with higher velocity ranges, the drift of the zero point and thermal convection associated with the anemometer itself may cause significant measurement errors. Hence, anemometers used for observation or monitoring of indoor airflow must be calibrated with sufficient accuracy. The calibration of the anemometers is, in most cases, conducted by facilities owned by calibration laboratories or manufacturers [1–4]. However, it takes a long time to calibrate even one anemometer.

Since January 2020, when the first person infected by SARS-CoV-2 was confirmed, the number of infected people has been increasing in Japan. Indoor spaces, such as houses and restaurants, were particularly prone to infection [5–7]. One reason for the spread of the virus is assumed to be the diffusion of the virus caused by indoor airflow. Because the virus is carried to the downstream side of the indoor airflow, the virus may diffuse over a social distance [8–10]. To determine the location of the downstream side and understand the local velocity distribution, the indoor airflow should be evaluated.

Velocity measurement is conducted at various companies, such as those making air conditioners, in order to

clarify the indoor airflow. For example, velocity measurements have been conducted in cleanrooms, in experimental draft chambers, and in local ventilation equipment. Since the size and airflow control system in such spaces are standardized, the velocity measurement method for these spaces can also be standardized [11–13]. However, it is difficult to apply the same velocity measurement method to indoor spaces such as houses or restaurants. These spaces have several variations, for example, the size of the spaces is not the same, various HVAC systems are installed, and the location of furniture is not fixed. Hence, in order to clarify the indoor airflow in various spaces, several anemometers should be placed over the entire space. Since it takes long time to calibrate a number of anemometers, equipment that can perform this task in a short amount of time is required.

The authors have developed a new wind tunnel that is compact and can calibrate an anemometer in a short time. Since the wind tunnel is a set of commercially available products, the assembly time is short, and the cost is not high. A stable and constant airflow in the range of approximately 0.2 to 0.6 m/s can be produced in the test section of the wind tunnel in order to evaluate anemometers used for monitoring indoor airflow. Since uniform airflow can be generated over the entire test section, several anemometers can be calibrated simultaneously.

*Corresponding author, E-mail: a.iwai@aist.go.jp

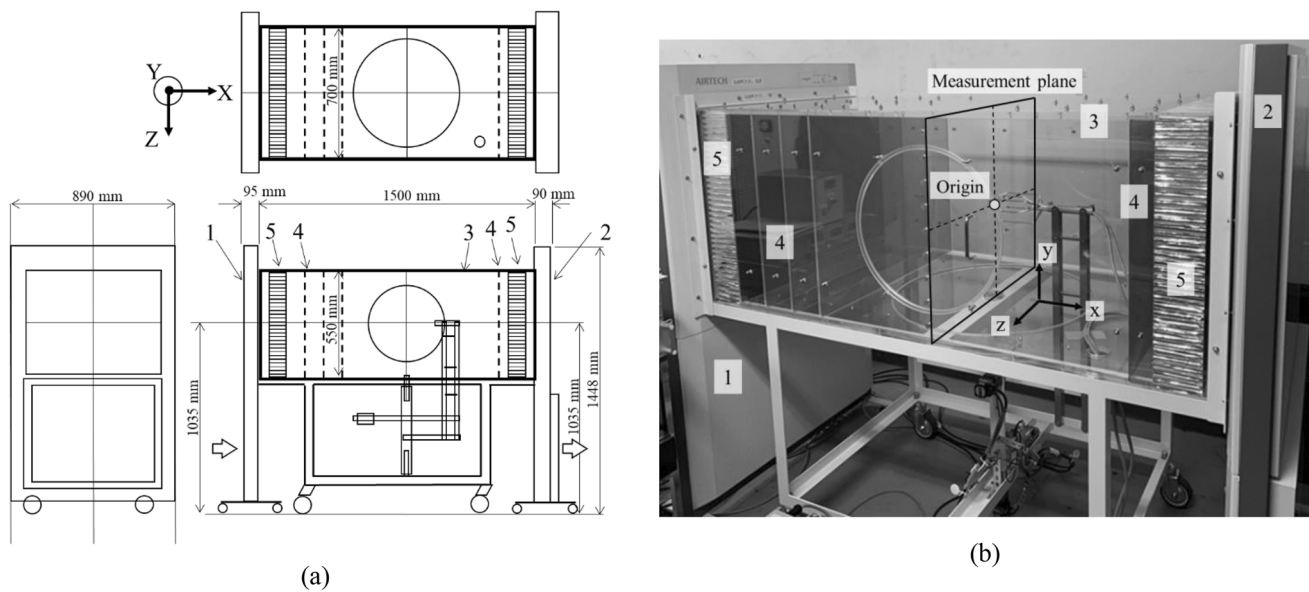


Fig. 1 Overview of wind tunnel. **a** Schematic diagram. **b** Photograph

In the present paper, the design concept for the wind tunnel, the specifications and requirements of the experiment, and the experimental verification are described.

2. Design Concept for Wind Tunnel

There are two requirements that the wind tunnel must satisfy. First, the accuracy of the velocity produced by the wind tunnel must be higher than that of anemometers commonly used. The accuracy of an anemometer for indoor airflow measurement is generally 30–50% [14]. Hence, the target accuracy of the wind tunnel is set as 10% [15].

Second, the calibration time using the wind tunnel is expected to be shorter than that using a calibration facility. In order to shorten the settling time from start-up until the airflow is stabilized, a pair of clean partitions with an air filter is used as a fan and a settling device for the wind tunnel. A filter having a high air-pressure loss, called a high-efficiency particulate air (HEPA) filter, is used instead of a nozzle and is able to alleviate instability in the flow and vortices caused by the fan. Moreover, since the clean

partition is thin in the streamwise direction, the wind tunnel is very compact.

Figure 1 and Table 1, respectively, show a schematic diagram and a component list of the wind tunnel. A horizontal flow is formed by the clean partitions. A push flow is produced by the clean partition on the upstream side across the air filter. A pull flow is produced by the clean partition on the downstream side to diminish stagnation in the downstream area and secondary flow behind the anemometer. The air speed controller for the clean partitions was modified using an inverter device so that the revolution of the fan could be adjusted in a stepless manner.

The test section was enclosed by clear acrylic boards. The length of the test section in the streamwise direction was 1500 mm. A closed test section was adopted to diminish disturbances due to indoor ventilation airflow or human movement. The measurement plane was rectangular, 700 mm in the spanwise direction and 550 mm in the vertical direction, and was defined as being at the 750 mm position in the streamwise direction from the upstream partition. The origin was located at the center of the measurement plane, and the x , y , and z axes were set as the

Table 1 Component list for wind tunnel

No	Name	Material	Quantity	Content
1	–	–	1	ACP-897AH (AIRTECH JAPAN, Ltd.) [16]
2	Clean partition	–	1	ACP-897CH (AIRTECH JAPAN, Ltd.) [16]
3	Test section	Acrylic	1	t5
4	Screen meshes	SUS	4	40#
5	Honeycomb cores	Aluminum	2	AL1/8-

streamwise, vertical, and span directions, respectively, as shown in Fig. 1. Screen meshes and honeycomb cores were placed on both the upstream and downstream sides of the test section to produce a uniform flow. Since the increase in temperature caused by the fan on the upstream side was negligibly small, the flow rates in the test section were assumed to be constant during the measurement. For effective accuracy evaluation, periodic calibration of the wind tunnel by the calibrated anemometer is desirable.

3. Evaluation of Wind Tunnel

3.1. Evaluation Index

In the present study, the performance of the wind tunnel was evaluated by two indices: the streamwise velocity and the combined velocity. These indices are important in order to evaluate the performance of both anemometers, the sensitivities of which are unidirectional and omnidirectional.

The streamwise velocity is indicated by V_x , and the combined velocity is determined by the following equation:

$$V = \sqrt{V_x^2 + V_y^2 + V_z^2}, \tag{1}$$

where V_y and V_z indicate the vertical velocity and the spanwise velocity, respectively.

The temporal performance of the wind tunnel was evaluated by estimating the average time per measurement point, and the settling time from start-up until the airflow was stabilized. The spatial performance was evaluated from the spatial distribution of the velocities and the blockage effect caused by the anemometer placement. These evaluations make it possible to operate the wind tunnel precisely and efficiently.

An ultrasonic anemometer WA-790 connected to a TR-90 T probe (Sonic Corporation) was used for this purpose. The anemometer was calibrated at the low-air speed standard calibration facility of the National Metrology Institute of Japan (NMIJ) in advance [3, 17]. The output frequency and resolution of the anemometer were 10 Hz and 0.005 m/s, respectively. The anemometer was placed such that the center of its sensing area was located on the measurement plane.

3.2. Average Velocity at the Origin

A certain averaging time is required to obtain a reliable velocity on the measurement plane. An experiment to find the optimal averaging time was conducted. The anemometer was placed so that the center of its sensing

area was located at the origin. The fan controller of the wind tunnel was varied from 30 to 100% in 10% steps, i.e., at eight points. By varying the averaging time from 10 to 60 s in 10 s steps, the average velocities were measured for each controller setting. The fan controller settings of 10% and 20% were not used due to the instability of the inverter controller of the fan.

In the present paper, we considered that a 60 s averaging time was sufficient to obtain a reliable and stable streamwise velocity, so that this value was defined as the reference value. The deviation of the streamwise velocity for each averaging time from the reference value is shown in Fig. 2. The calibration and measurement capability (CMC) of the low-air speed standard set by NMIJ [17] is indicated with dashed lines. Even for the shortest averaging time of 10 s, the deviations were considerably smaller than the CMC, and 10 s was therefore considered to be sufficient for the measurement time using the wind tunnel.

The velocities at the origin were observed for each fan controller setting. The average velocity in each direction is shown in Fig. 3. The average streamwise velocity V_x was approximately 0.2 m/s at a fan setting of 30% and was approximately 0.6 m/s at a fan setting of 100%. The velocities in the y and z directions, V_y and V_z , respectively, were less than ± 0.06 m/s for all velocity ranges. The standard deviations of the average velocities in each direction were less than 0.005 m/s, which is the same level as for commercial low-speed wind tunnels [18]. Moreover, the streamwise velocity V_x was approximately proportional to the fan controller setting, indicating that this wind tunnel can be operated easily. From the data, it was cleared that

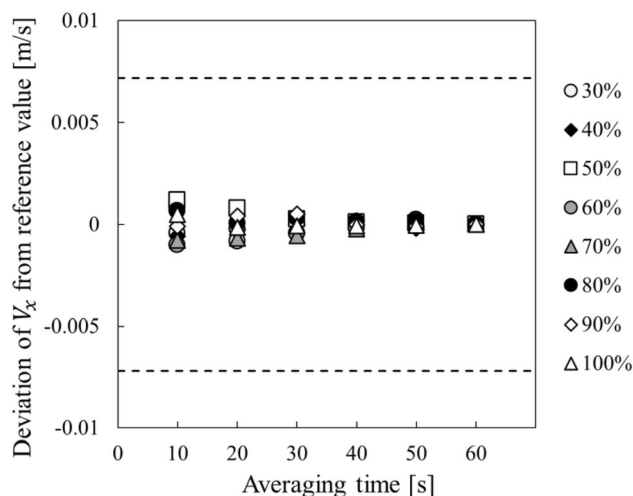


Fig. 2 Deviation of streamwise velocity from reference value. The dashed lines indicate the calibration and measurement capability (CMC) of the low-air speed standard set by the National Metrology Institute of Japan (NMIJ)

the desired reference air speed at Origin can be achieved simply by adjusting the fan setting.

Next, the ratio of V to V_x is shown in Fig. 4. The dashed line indicates the CMC of the low-air speed standard set by the NMIJ [17]. Although a 2% difference was observed between V and V_x at a fan setting of 30%, these values can be regarded as equivalent because the difference was smaller than the CMC value.

3.3. Settling Time from Start-Up of Wind Tunnel

The settling time was evaluated from start-up of the wind tunnel until the airflow was stabilized. The instantaneous streamwise velocity at the origin from the start-up to 60 s is shown in Fig. 5. The fan controller of the wind tunnel was set at 30%, 50%, and 100%. In the cases in which the fan controller was set at 30% and 50%, the instantaneous V_x 30 s from start-up was stable at the set air speed. Although overshoot occurred at the 100% fan setting, the instantaneous V_x after 50 s was stable. After 60 s had passed from start-up, no drift was observed in the instantaneous V_x for any fan setting. Having no drift means that the airflow is adapted for the evaluation of the anemometer.

3.4. Spatial Distribution of Velocity

The velocity components in each direction, V_x , V_y , and V_z , on the measurement plane were investigated in order to confirm the area where the velocity profile can be considered to be uniform. The ultrasonic anemometer used as a reference in this paper has high sensitivity and high accuracy in the low-air speed range and can measure three-dimensional velocity. Besides, the ultrasonic anemometer

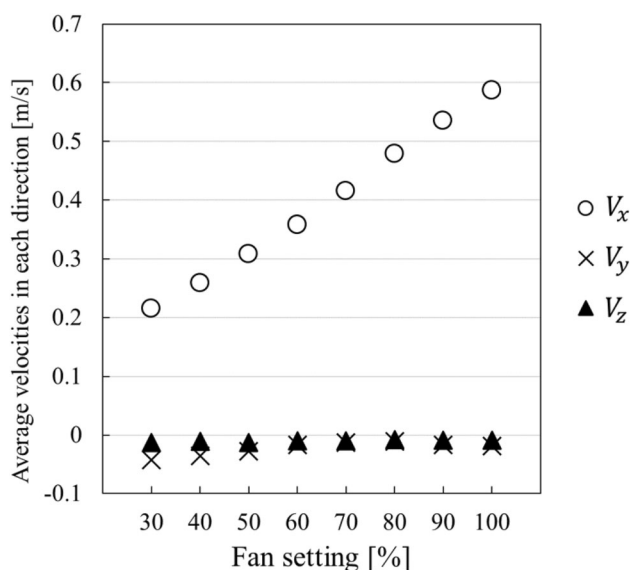


Fig. 3 Average velocities in each direction at origin

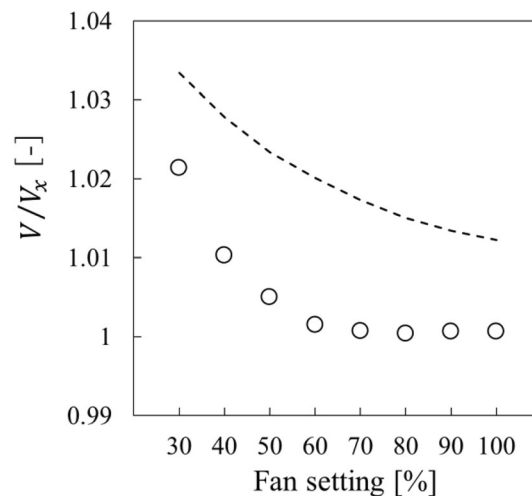


Fig. 4 Ratio of air speed to streamwise velocity. The dashed line indicates the CMC of the low-air speed standard

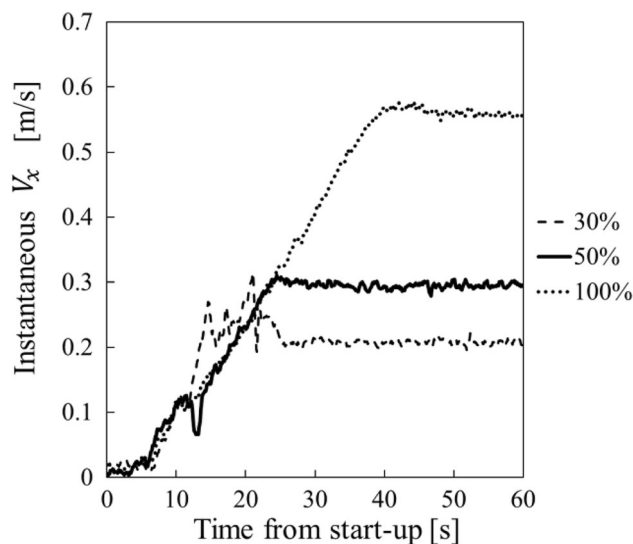
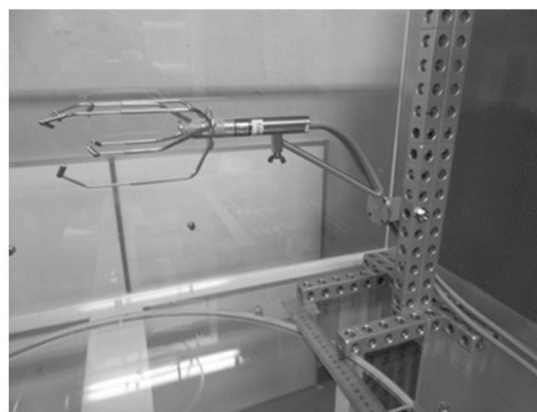
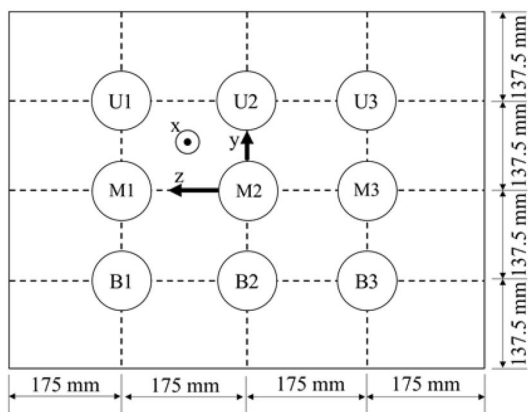


Fig. 5 Instantaneous streamwise velocity at origin

yields little effect on the distribution of velocity although its physical dimension is large. The measurement points were set at every 1/4 of the total distance in the y and z directions on the measurement plane, i.e., nine points in total. The locations of the measurement points and their identifications are shown in Fig. 6a, and the fixture used for this measurement is shown in Fig. 6b. The measurement point labeled M2 is the origin. The air flows from the back side to the front side in this figure. The average velocity over 10 s at each measurement point was measured after the flow had settled. The reproducibility of the average velocity at M2 was comparable with the CMC.

The ratio of V_x with respect to that at the origin M2 is shown in Fig. 7. In the range where the streamwise velocity is more than 0.4 m/s, the ratio was less than 5% at



(a)

(b)

Fig. 6 a Location of measurement points. b Fixture

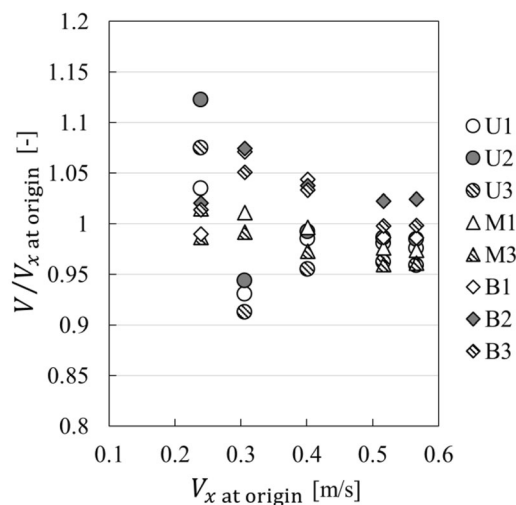
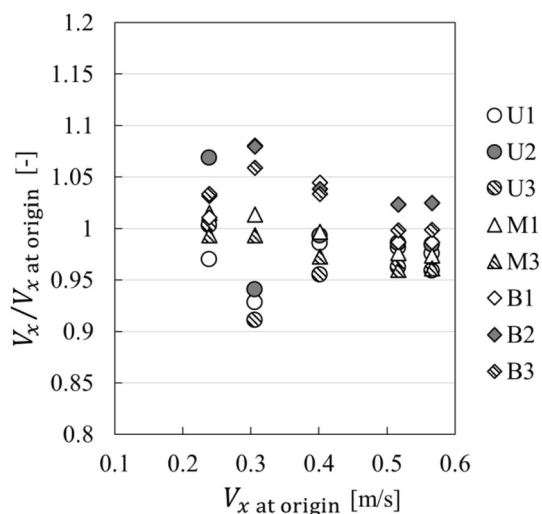


Fig. 7 Ratio of streamwise velocity on measurement plane against that at origin

Fig. 8 Ratio of air speed on measurement plane against that at the origin

all measurement points. Even at 0.3 m/s, where the scattering of the spatial distribution is the largest, the deviation is at most $\pm 10\%$. At the middle points in the vertical direction, M1 and M3, the deviations were less than 5% at all air speed settings.

Hence, for the case in which the unidirectional anemometer is evaluated and a precision of better than 5% is required at all air speed settings, the sensor unit of the anemometer should be located at the middle points in the y direction on the measurement plane. On the other hand, for the case in which a precision of 10% for evaluation of a unidirectional anemometer is sufficient, the sensor unit of the anemometer may be placed at any measurement point on the measurement plane.

Next, the ratio of V with respect to that at the origin M2 is shown in Fig. 8. Whereas this figure exhibits a trend that is similar to that in Fig. 7, the deviation of V in Fig. 8 due

to the measurement point being different was larger than V_x at 0.2 m/s and 0.3 m/s. There was a measurement point at which V exceeds 10% of that at point M2. At the middle points in the y direction, M1 and M3, the deviations were less than 5% at all air speed settings.

In conclusion, for cases in which an omnidirectional anemometer is being evaluated when a better than 5% precision is required at all air speed settings, the sensor of the anemometer should be located in the middle point in the y direction on the measurement plane. When a 10% precision is acceptable, the sensor of the anemometer may be placed at any measurement point on the measurement plane.

3.5. Blockage Effect

In this section, the velocity variation caused by a blockage was evaluated in order to evaluate the flow when more than

one anemometer is located on the measurement plane. Evaluation of the blockage effect is essential when calibration is conducted because a wind tunnel having a closed test section is sensitive to blockages [19–21]. A rectangular plate resembling the anemometer was placed in the wind tunnel, and the velocity at the origin was measured. The reason for adopting the rectangular plate is that it was planned to ensure that the flow is blocked, and the blockage effect is maximized. We evaluated an index indicating whether the blockage effect is sufficiently small, and additional anemometers can be located on the measurement plane.

The blockage effect of the block in the test section is the change in the velocity profiles on the measurement plane caused by the decrease in the effective cross-sectional area and the non-homogeneity of the flow profiles. The influence of the blockage effect differs depending on the shape and size of the block. Nevertheless, the decrease in the effective cross-sectional area, which is considered to be the largest factor, was evaluated. The cross section and thickness of the block are $0.15\text{ m} \times 0.125\text{ m}$ and 0.025 m , respectively. This cross-sectional area is approximately 5% of that of the measurement plane. This blockage ratio is larger than that for most commercial anemometers used for indoor flow.

An overview of the evaluation and a photograph is shown in Fig. 9. The anemometer was placed at the origin. The block was located at either d1 or d2, which are the middle points between the anemometer and the side wall.

The ratio of V_x with and without the block at the origin point is shown in Fig. 10. The solid line indicates the velocity theoretically corrected by the cross-sectional area. The ratio of V_x agreed with the theoretical value. Almost the same result was observed for the ratio of V .

Based on these results, by applying the correction of the cross-sectional area, if more than one anemometer is placed in the wind tunnel and the blockage ratio for the

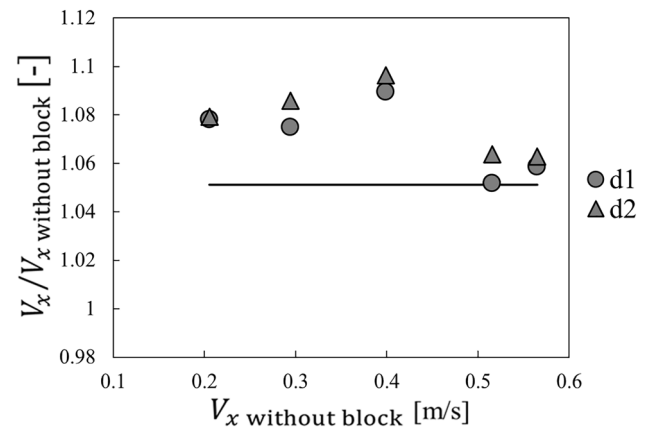


Fig. 10 Ratio of streamwise velocity with and without block. The solid line indicates the velocity theoretically corrected by the cross-sectional area

total blockage for all the anemometers is less than 5%, then, evaluation of all the anemometers can be performed at the same time because the deviation of the corrected velocity is negligibly small. In general, thermal and ultrasonic anemometers for indoor airflow have a less than 5% blockage ratio with respect to the cross section of the measurement plane. We are confident that this wind tunnel can evaluate anemometers in a short measurement time with a sufficiently high precision and will be useful for taking preventative measures against infectious diseases.

The solid line indicates the velocity theoretically corrected by the cross-sectional area.

4. Conclusion

A compact wind tunnel was developed for the quick evaluation of anemometers used to measure indoor airflow. This wind tunnel is composed of a clean partition with an air filter that has high pressure loss and various

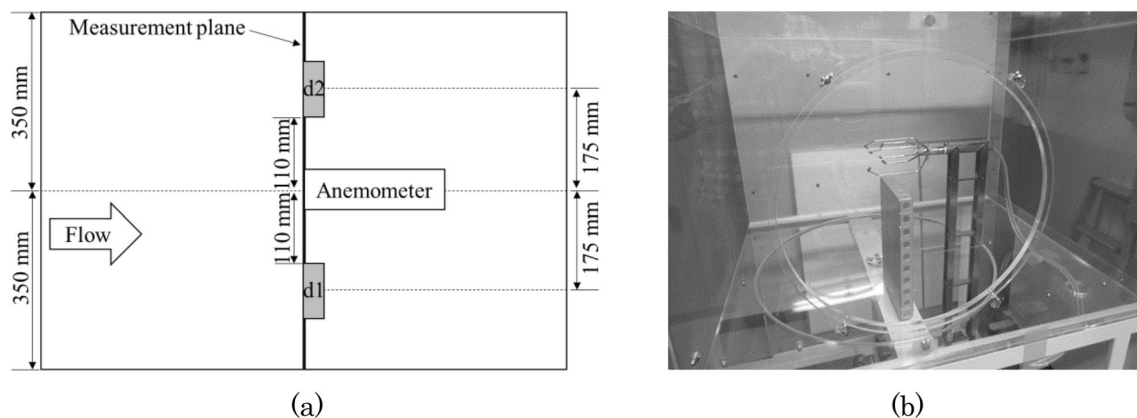


Fig. 9 Overview of the evaluation method for the blockage effect. **a** Schematic diagram. **b** Photograph

commercially available devices. The temporal and spatial performance of the wind tunnel, which can be described by several indices, including averaging time, settling time, spatial distribution of the velocity, and the blockage effect, was examined on the measurement plane. An averaging time of 10 s was found to be sufficient, and the airflow was confirmed to be stable after 60 s from the start-up of the wind tunnel. A streamwise velocity of approximately 0.2 to 0.6 m/s can be produced, and the ratio of V to V_x can be regarded almost the same. Regardless of whether the anemometers are unidirectional or omnidirectional, the anemometer sensors should be located at the middle points in the vertical direction on the measurement plane in order to evaluate the anemometers at a precision of greater than 5%. In addition, the increase in velocity due to the blockage effect caused by additional anemometers approximately agrees with the theoretical value.

We are confident that this wind tunnel can evaluate anemometers in a short measurement time with a sufficiently high precision and hence, can contribute to the understanding of the indoor airflow. In the future, the relation between the number and the layout of the anemometers and measurement precision will be investigated.

Acknowledgements This research was supported by AMED through Grant Number JP20he0722012. The authors would like to thank Tsukuba Rikaseiki Co., Ltd. for providing technical information and support for the wind tunnel and Mr. Toru Hirayama (technical staff at NMIJ) for collecting the experimental data.

References

- [1] S. Pezzotti, J.I. D'Iorio, V. Nadal-Mora and A. Pesarini, A wind tunnel for anemometer calibration in the range of 0.2 m/s -1.25 m/s. *Flow Measurement and Instrumentation*, **22** (2011) 338–342.
- [2] A. Piccato, R. Malvano and P.G. Spazzini, Metrological features of the rotating low-speed anemometer calibration facility at INRIM. *Metrologia*, **47**(1) (2009) 47.
- [3] Y. Terao, M. Takamoto and T. Katagiri, Very low speed wind tunnel for Anemometer calibration. *Journal of JSME B*, **63**(607) (1997) 192–197 (Japanese).
- [4] H. Müller, I. Caré, P. Lucas, D. Pachinger, N. Kurihara, C. Lishui, C.M. Su, I. Shinder and P.G. Spazzini, CIPM key comparison of air speed, 0.5 m/s to 40 m/s (CCM-FF-K3.2011). *Metrologia*, **54** (2017) 07013.
- [5] R.C. Law, J.H. Lai, D.J. Edwards and H. Hou, COVID-19: research directions for non-clinical aerosol-generating facilities in the built environment. *Buildings*, **11**(7) (2021) 282.
- [6] D.A. Edwards, D. Ausiello, J. Salzman, T. Devlin, R. Langer, B.J. Beddingfield, A.C. Fears, L.A. Doyle-Meyers, R.K. Redmann, S.Z. Killeen and N.J. Maness, Exhaled aerosol increases with COVID-19 infection, age, and obesity. *Proceedings of the National Academy of Sciences of the United States of America*, **118**(8) (2021) 1–6.
- [7] S.E. Hwang, J.H. Chang, B. Oh and J. Heo, Possible aerosol transmission of COVID-19 associated with an outbreak in an apartment in Seoul Korea, 2020. *International Journal of Infections Diseases*, **104** (2021) 73–76.
- [8] M.A. Kohanski, L.J. Lo and M.S. Waring, Review of indoor aerosol generation_ transport_ and control in the context of COVID-19. *International Forum of Allergy & Rhinology* **10** (10), 1173–1179.
- [9] R.K. Bhagat, M.D. Wykes, S.B. Dalziel and P.F. Linden, Effects of ventilation on the indoor spread of COVID-19. *J. Fluid Mech.*, **903**(F1) (2020) 1–18.
- [10] E. Light, J. Bailey, R. Lucas and L. Lee, HVAC and COVID-19: filling the knowledge gaps. *ASHRAE Journal*, **62**(9) (2020) 20–28.
- [11] ANSI/ASHRAE 110–1995(1995).
- [12] EN14175–3 Fume cupboards – Part 3: type test methods (2019).
- [13] ISO14644–3, Cleanrooms and associated controlled environments – Part 3: test methods (2019).
- [14] Y. Terao, M. Takamoto and T. Katagiri, Reliability of commercially available air flow velocimeters, *Transactions of the Society of Instrument and Control Engineers*, **28** (3) (1992) (Japanese).
- [15] ISO7726 Ergonomics of the thermal environment – instruments for measuring physical quantities (1998).
- [16] Catalog of clean partitions, <https://www.airtech.co.jp/products/cleaneq/1064/> (Accessed on 03 Oct 2022) (Japanese).
- [17] Bureau international des Poids et Mesures (BIPM), Key comparison database, Appendix C, CMCs (online), (Accessed on 11 May 2022).
- [18] Wind tunnel database in Japan, <http://www.jamstec.go.jp/ceist/kazenagare-pf/windtunnel-db/> (Accessed on 11 May 2022) (Japanese).
- [19] W. Juan and C.H. Ann, Blockage effects in the calibration of anemometer in a wind tunnel, 15th flow measurement conference (2010), 1–10.
- [20] I. Care and M. Arenas, On the impact of anemometer size on the velocity field in a closed wind tunnel. *Flow Measurement and Instrumentation*, **44** (2015) 2–10.
- [21] J. Geršl, P. Busche, M. de Huu, D. Pachinger, H. Müller, K. Hölper, A. Bertašienė, M. Vilbaste, I. Care, H. Kaykısızlı and L. Maar, Comparison of calibrations of wind speed meters with a large blockage effect. 18th flow measurement conference (2019), 1–9.

Publisher's Note Springer Nature remains neutral with regard to jurisdictional claims in published maps and institutional affiliations.

Springer Nature or its licensor (e.g. a society or other partner) holds exclusive rights to this article under a publishing agreement with the author(s) or other rightsholder(s); author self-archiving of the accepted manuscript version of this article is solely governed by the terms of such publishing agreement and applicable law.